



HAL
open science

A Brownian motion technique to simulate gasification and its application to C/C composite ablation

Jean Lachaud, Gerard L. Vignoles

► **To cite this version:**

Jean Lachaud, Gerard L. Vignoles. A Brownian motion technique to simulate gasification and its application to C/C composite ablation. *Computational Materials Science*, 2008, 44 (4), pp.1034-1041. 10.1016/j.commatsci.2008.07.015 . hal-00410192

HAL Id: hal-00410192

<https://hal.science/hal-00410192>

Submitted on 11 Sep 2023

HAL is a multi-disciplinary open access archive for the deposit and dissemination of scientific research documents, whether they are published or not. The documents may come from teaching and research institutions in France or abroad, or from public or private research centers.

L'archive ouverte pluridisciplinaire **HAL**, est destinée au dépôt et à la diffusion de documents scientifiques de niveau recherche, publiés ou non, émanant des établissements d'enseignement et de recherche français ou étrangers, des laboratoires publics ou privés.



Contents lists available at ScienceDirect

Computational Materials Science

journal homepage: www.elsevier.com/locate/commatsci

A Brownian motion technique to simulate gasification and its application to C/C composite ablation

J. Lachaud *, G.L. Vignoles

University of Bordeaux 1, Laboratoire des Composites ThermoStructuraux (LCTS) 3, Allée de La Boétie, 33600 Pessac, France

ARTICLE INFO

Article history:

Received 28 March 2008
Received in revised form 7 July 2008
Accepted 15 July 2008
Available online xxxx

PACS:

87.10.Rt
05.40.Jc
81.65.Mq
68.35.Ct
68.35.Fx
72.80.Tm

Keywords:

Brownian motion
Sticking event
Receding surfaces
Carbon–carbon composites

ABSTRACT

Ablation of carbon–carbon composites (C/C) results in a heterogeneous surface recession mainly due to some gasification processes (oxidation, sublimation) possibly coupled to bulk mass transfer. In order to simulate and analyse the material/environment interactions during ablation, a Brownian motion simulation method featuring special Random Walk rules close to the wall has been implemented to efficiently simulate mass transfer in the low Péclet number regime. A sticking probability law adapted to this kind of Random Walk has been obtained for first-order heterogeneous reactions. In order to simulate the onset of surface roughness, the interface recession is simultaneously handled in 3D using a Simplified Marching Cube discretization. This tool is validated by comparison to analytical models. Then, its ability to provide reliable and accurate solutions of ablation phenomena in 3D is illustrated.

© 2008 Published by Elsevier B.V.

1. Introduction

Carbon/carbon (C/C) composites, which keep excellent mechanical properties at high temperatures [1], are used as thermostructural protections in various applications such as atmospheric reentry (vehicle thermal protection systems) [2], propulsion (rocket nozzle) [3], and experimental Tokamak reactors for nuclear fusion (divertor and first wall armor) [4]. In these applications, the C/C composites are mainly ablated by some gasification processes (oxidation, sublimation) [2]. An efficient design of a thermostructural protection relies on an accurate evaluation of the wall recession caused by ablation. In particular, C/C composites develop surface roughness features, which may display a strong coupling with the surrounding environment [5,6]. The surface roughness chiefly arises from the heterogeneity of the composites, whose fibers and matrices are made of distinct forms of carbon [7]. In a previous work, the composite behavior has been analytically modeled in steady state [6]. The results were in agreement with the experi-

mental observations [7] and provided a good understanding of C/C composite behavior during ablation. Nevertheless, in order to enable an analytical modeling, the composite architecture had been simplified as much as possible. Mainly, as a first approximation, the fiber section had been considered circular, while the actual section outline slightly undulates around a mean circular line. Moreover, a 3D modeling of the transient behavior cannot be attained through purely analytical methods. This paper aims to present a 3D numerical simulation tool implemented to model with more accuracy C/C composites and their surface roughening during ablation.

Physico-chemical ablation, studied at microscopic scale, typically belongs to heterogeneous reaction/mass transfer problems with a receding surface [2,6,8,9]. The dynamics of nontrivial pattern formation at small scales poses a serious challenge for numerical simulations. A precise integration of the equation of surface motion at the pattern scale is mandatory. For instance, Finite volumes/volume-of-fluid methods represent one possible solution for this type of problems, and are quite efficient for most of the cases [10]; but they may be extremely memory-consuming as soon as large images with possibly complicated patterns are to be dealt

* Corresponding author. Tel.: +33 650 265 8474; fax: +33 0 5 56 84 12 25.
E-mail address: jean.lachaud@gadz.org (J. Lachaud).

with. A multigrid approach may be a solution to this inconvenient, since the gas concentration field, some distance away from the surface undergoes small 3D gradients compared to the surface. Another way to tackle this problem is to use a Random Walk description of mass transfer: this method is known to provide excellent results when computing effective transport coefficients, *i.e.* only an average gas behavior, inside large and complex 3D images of porous media [11]. Random Walk methods are available for the simulation of either continuum [12], transition or rarefied gas transport [13]. However, the algorithms have to be extended in order to account for the heterogeneous reaction. One of the solutions proposed in the past rests on the coupling of the Random Walk code far from the surface with a Finite-Difference solver close to it [14]. Here it is chosen to address the gas–solid reaction directly through the use of a suited sticking probability law. This represents a lighter algorithm, and allows to handle easily the surface evolution, thanks to a simplification of the Marching Cube method [15] for the surface discretization.

In the first section, the mathematical form of the studied problem is presented. In the second section, the numerical tool itself is presented and validated by comparison to the analytical solution obtained in [6], in the case of circular fibers. In the last section, an ablation simulation is carried out on a realistic fiber section and compared to experimental observations of surface roughness features.

2. Model and analytical solution

2.1. Ablation model

The ablation process leads to the recession of the material surface S under heterogeneous gasification processes, like oxidation or sublimation [2]. The macroscopic motion of this surface can be interpreted as an advancing wavefront. The surface position may be described in Cartesian coordinates by the following scalar equation:

$$S(x, y, z, t) = 0 \quad (1)$$

such that the function S , which possesses first-order partial derivatives almost everywhere, acquires nonzero values at all points not lying on the interface [16]. This equation may be derived with respect to time

$$\frac{\partial S}{\partial t} + \mathbf{v} \cdot \nabla S = 0 \quad (2)$$

where $\mathbf{v} = v/\mathbf{n}$ is the surface local normal velocity, with v the local solid molar volume of the ablated material [16]. In the case of heterogeneous materials, v varies with space. J (in $\text{mol m}^{-2} \text{s}^{-1}$) is the molar rate of ablation. In this work, it is assumed to follow a first order kinetic law for oxidation and a Knudsen–Langmuir model for sublimation [2,17]. The Péclet mass number is low close to the wall [7,17]. Under these hypotheses, oxidation and sublimation are shown to be mathematically equivalent as far as gasification and mass transfer are concerned [2,17]. Using oxidation notations, the model writes

$$J = -D\nabla C \cdot \mathbf{n} = -k \cdot C(S = 0) \quad (3)$$

where k (in m s^{-1}) is the gasification rate of the material (like v , k is a function of space for heterogeneous materials), D (in $\text{m}^2 \text{s}$) the diffusion coefficient of the reactant in the bulk fluid phase, and $C(S = 0)$ (in mol m^{-3}) is the reactant gas concentration at the material surface. Mass conservation of the reactant in the fluid writes

$$\frac{\partial C}{\partial t} + \nabla \cdot (-D\nabla C) = 0 \quad (4)$$

Boundary conditions for concentration relative to the model domain have to be specified (see for example Fig. 1a). A Dirichlet condition ($C = C_0$) on the boundary layer top is shown to be suitable [6]. On lateral boundaries, a periodicity condition is retained. The interface position S as a function of space and time is then given by the simultaneous resolution of Eqs. (2) and (4). For heterogeneous materials, this model cannot be solved analytically in the general case.

2.2. An analytical solution

Let the analytical solution previously obtained for circular fibers [6] be briefly recalled here since it is a perfect reference case for the following 3D validation of a the simulation tool (see Section 3.2). The general model of Section 2.1 has been applied to the cell represented on Fig. 1aa. It represents a carbon fiber embedded in a carbon matrix shown before ablation: the surface is initially flat (no surface roughness). Translation conditions on lateral boundaries and the Dirichlet condition ($C = C_0$) on boundary layer top are imposed. Under these boundary conditions, the cell represents a composite yarn, whose lateral extension is infinite, and ablated perpendicularly to its principal direction. Both components are gasified by a first-order reaction (oxidation of carbon by oxygen for example), the matrix being more reactive than the fibers [7]. The concentration gradient of reactant in the fluid phase has been shown to be vertical in steady state [6], that is, along z (see Fig. 1a). An analytical solution to this problem gives the following results [17,6]: (i) Due to the higher recession rate of the matrix, the fibers are partially stripped, become thinner, and acquire a needle shape. (ii) Only two parameters are necessary to describe the steady state surface roughness features of the yarn: a reactivity contrast A and a Sherwood number Sh . The reactivity contrast between the matrix and the fibers A is given by

$$A = \frac{k_m v_m}{k_f v_f} \quad (5)$$

where k_m , v_m , k_f , and v_f are, respectively, the matrix and fiber reactivities and solid molar volumes, which are assumed constant for each phase. For the standard composites and according to literature data, fiber and matrix densities are of the same order of magnitude, while matrices are neatly more reactive than fibers; hence, one has $A > 1$ [7]. The geometry of the steady state is strongly linked to this contrast; the higher it is, the higher the denuded fiber size h_f^s (from fiber tip to matrix level) is when steady state is reached. The Sherwood number Sh writes

$$Sh = \frac{k_m R_f}{D} \quad (6)$$

where R_f is the fiber radius. It is an indicator of the three reaction regimes that can appear on this heterogeneous reactive surface: a diffusion-limited regime ($Sh \gg 1$), a transition regime ($Sh \sim 1$), and a reaction-limited regime ($Sh \ll 1$). For small values of Sh , the fiber tip geometry is conical and only depends on A , with $h_f^s = R_f \sqrt{A^2 - 1}$ (see Fig. 1b). When Sh increases but is lower than $\sqrt{A^2 - 1}$, diffusional effects tends to lower h_f^s and the fiber tips become ogival. For higher values of Sh , fibers tips display a plateau and $h_f^s = R_f(A - 1)/Sh$. Hence, in diffusion-limited regime, h_f^s tends towards zero.

This analytical model seems then of great interest for a validation of the numerical simulation tool, as well as for the diffusion and reaction part (all reaction/diffusion regimes are scanned) than for the front tracking because 3D surfaces including singularities (fiber tips) are featured.

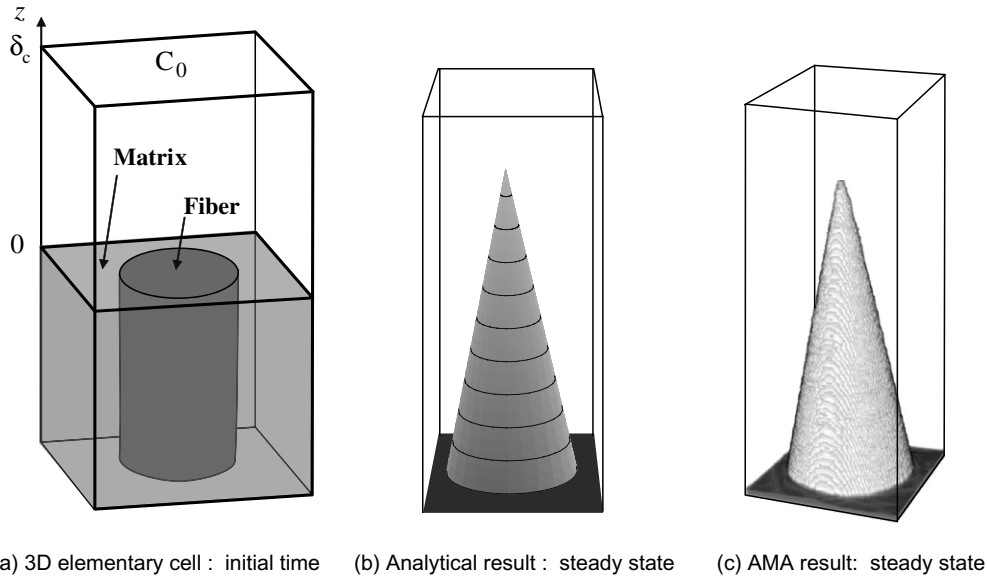


Fig. 1. Validation of AMA by comparison to a 3D analytical model in reaction-limited regime ($A = 5$).

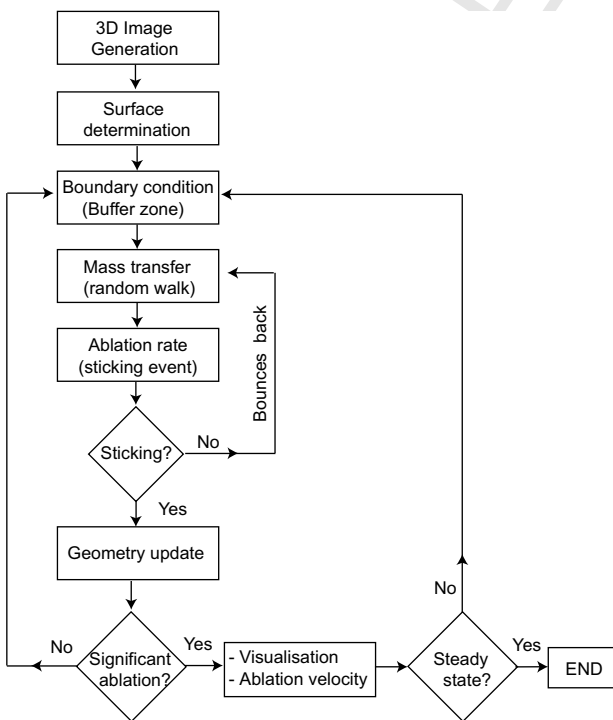
3. Numerical solution

AMA has been developed on a Monte-Carlo Random-Walk principle [18–23]. AMA is the acronym for: *Ablation Marches Aléatoires* (Random Walk Ablation in French).

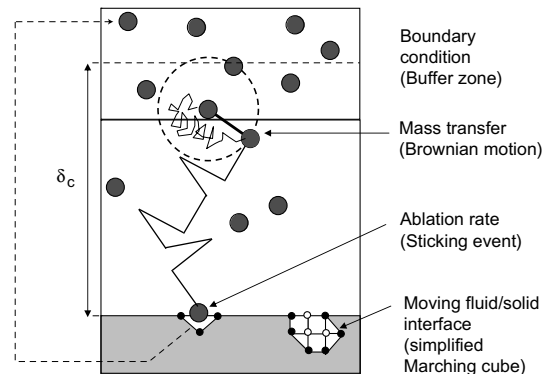
3.1. AMA algorithm presentation

A scheme of the general algorithm and a sketch of AMA main features are presented on Fig. 2a and b. First, a 3D image containing

several phases (fluid/solids) is generated. It is discretized as grey-scale values on a 3D cubic grid. Then, the fluid/solid interface (Eq. 1) is determined by a **Simplified Marching Cube** approach [20], which is a linear approximation of the actual surface in each voxel (3D pixel) of the interface. Mass transfer from the bulk gas to the wall (Eq. 4) is simulated by a **Random Walk** based on the Brownian motion simulation technique, which is a continuum (grid-free), rapidly converging and memory-sparing method for diffusion in a continuous fluid [18]. In order not to degrade the numerical accuracy of the method, it is most convenient to give a



(a) Scheme of AMA algorithm



(b) Sketch of AMA principle

Fig. 2. Schematic description of AMA.

constant representativeness to each **Random Walker** (i.e. a constant number of actual gas molecules associated to each walker). In addition, one has to satisfy the Dirichlet boundary condition on the upper part of the fluid phase. This is achieved through the use of a buffer zone in which a constant number of walkers is ensured. The total number of walkers in the rest of the fluid phase results from the diffusion/reaction process, that is, the coupled resolution of Eqs. (3) and (4). As represented on Fig. 2b, the path followed by a walker is not the physical one dictated by gas kinetics, but another one based on Brownian motion simulation technique that requires less computational time [18]. One of the properties of Brownian motion is that, in average, the space increment Δr covered by a molecule is related to the time increment Δt by the following equation:

$$\Delta t = \frac{\Delta r^2}{6D} \quad (7)$$

where D is the diffusion coefficient. Using this property for simulation purpose, the size of the space increment has obviously to be chosen as large as possible to decrease the computational time, but small enough when compared to the characteristic size of the problem. A parametrical study must then be carried out to determine the relevant space increment; it is the equivalent of a mesh study for finite element methods. The trajectory of each walker is followed individually during a given time interval $\Delta t_e = N_s \Delta r$, where N_s is a chosen number of steps. The value of Δt_e is evaluated to ensure a walk duration leading to a probability of about 50% to hit a wall. In general, N_s is rather large. At each step, the walk direction is determined randomly and equiprobably in 3D space. The heterogeneous first-order reaction on the wall (Eq. 3) is simulated using a sticking event based method [19]. Let us assume that a walker hits the surface after a walk duration Δt_w ($0 < \Delta t_w < \Delta t_e$). A random number between 0 and 1 is generated from a uniform distribution. If that number is higher than a previously determined sticking event probability, the walker bounces back and its walk goes on until either it hits the wall again or Δt_e is reached. In the converse case, the walker is assumed to stick; another walker is released in the buffer zone, for a walk duration of only $\Delta t_e - \Delta t_w$. This ensures that in steady state conditions the flux received by the wall is equal to the flux entering the simulation box by its upper side.

Every sticking event is associated to the solid node which lies nearest to the exact location where it takes place. The amount of sticking events is recorded for every solid node of the fluid/solid interface. Whenever for a given node the cumulated number of sticking events reaches a given threshold, that is, when the required quantity of reactant to gasify one voxel is reached, it is converted into fluid. Then, the surface is modified and has to be updated (Eq. 2). When a significant number of solid voxels is turned into fluid, an image is recorded. When an appreciable number of fluid voxels has been created (say, the volume of one horizontal slice of the image), the resolution domain is shifted downwards by the corresponding amount (one voxel height), in order to preserve a constant fluid volume throughout the simulation. The average ablation velocity can be inferred using the frequency of geometry shifts. The average ablation velocity and reactant flux are compared with the value obtained at the previous geometry shift operation. When the flux is constant from one run to another, this means the steady state is reached, and then the simulation ends. The steady state may also be visualized by 3D rendering and characterized by image analysis. Let some critical steps of the algorithm be further detailed.

To handle accurately the Dirichlet boundary condition, a parameter variation study has shown that the size of the buffer zone should be at least twice as large as the space increment Δr of the **Random Walk**. As sketched on Fig. 2b, using a buffer zone, the boundary condition is applied in practice at a position Δr inside

that zone, the size of the concentration boundary layer δ_c being then obtained by the sum of the fluid phase height (buffer excluded) and Δr .

The choice of the space increment size is critical as far as accuracy and computational time are concerned. In the bulk fluid phase, Δr has to be taken as large as possible, in order to lower the computational time. Conversely, close to a wall, a parameter variation study has shown that Δr should be smaller than the characteristic size of the surface roughness (fiber radius in our case for example). Indeed, in the converse case, some zones may be numerically shaded. Moreover, some conditions have to be respected for the walker diffuse reflection to insure mass conservation. When a walker hits the wall, its last space increment Δr_w , which leads to collision, is smaller than Δr (or at most equal). In this algorithm, the walker bounces back according to a diffuse emission law (Knudsen's cosine law) with a space increment Δr_w . Using this bouncing rule, the average space increment size close to the wall automatically decreases, leading to a more accurate simulation of surface recession. Compared to finite element, this is the equivalent of an adaptative mesh refinement that follows the wall recession.

The heterogeneous first-order reaction on the wall is simulated by a sticking event with a probability P_s adapted to the Brownian motion simulation technique. By definition, the sticking probability is the ratio between the number of molecules that are consumed (or stuck) on the wall and the number of molecules hitting the wall. In term of molar fluxes, this writes [19]

$$\tilde{P}_s = \frac{\Phi_R}{\Phi_{MT} + \Phi_{MA}} \quad (8)$$

where $\Phi_R = Ck$ is the molar flux consumed on the wall. Φ_{MT} is the molar flux transported to the wall by mass transfer, which is equal to Φ_R in steady state (mass conservation). In the case of ablation or condensation, the solid surface velocity is slow compared to mass transport because of the low solid to gas molar volume ratio; hence, surface evolution and mass transport are decoupled and mass transport can be considered as a steady state phenomenon. Φ_{MA} is the molecular agitation flux. In the case of **Random Walks** following Maxwell distribution, this flux is called half Maxwellian flux and writes $1/4C\langle v \rangle$, where $\langle v \rangle$ is the molecular agitation mean velocity. The numerical velocity of a walker hitting the wall is $v = 6D/\Delta r_w$ (from Eq. 7). The mean quadratic length $\langle \Delta r_w \rangle$ is potentially a function of the surface roughness or the presence of notches. Therefore, to maintain the accuracy of the simulations in the case of complex geometries, it is important to keep Δr_w itself in the numerical method, the mean quadratic length being computed during the simulation. To account for the fact that the Brownian **motion Random Walk** implemented does not follow a Maxwellian distribution law, the introduction of a correction coefficient γ in the relation of the molecular agitation flux is **proposed**

$$\Phi_{MA} = 3/2\gamma CD/\Delta r_w \quad (9)$$

Combining Eqs. (8) and (9), P_s is found to write [24]

$$\tilde{P}_s = \frac{1}{1 + \frac{3\gamma D}{2k\Delta r_w}} \quad (10)$$

A numerical study is carried out in the validation section to validate the existence of γ for the **Random Walk** implemented and to assess its value.

For ablation study, the key outputs are the local surface recession, whose fluctuations lead to surface roughness, and the global ablation velocity. Since the molar volume of the material is low compared to the gas, the surface evolution is slow compared to gas diffusion. In actual experiments, a huge number of reactant

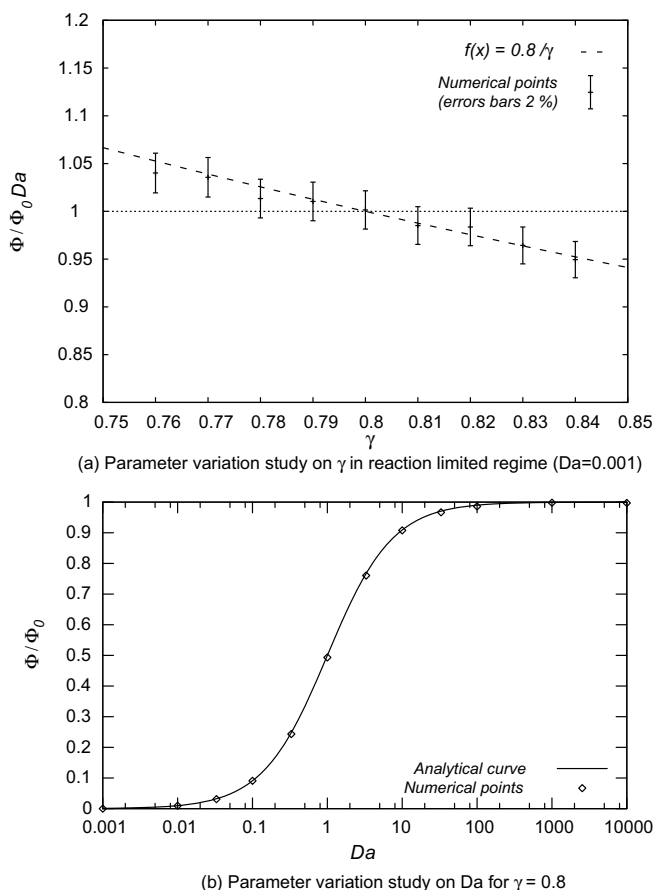


Fig. 3. AMA validation by comparison to a 1-D model ($\Phi_0 = DC_0/\delta_c$).

such a fine description, which fortunately is in no way necessary, especially in view of the discrete mode of geometry representation [19]. Then, the number of walkers can be restricted, using for each walker a representativeness of many reactant molecules estimated as follows. An elementary cube is assumed to be ablated when the corresponding number of sticking events reaches a given number N . N has to be chosen large enough so that statistical fluctuations are small, but is otherwise arbitrary. Theoretically, the statistical precision is roughly given by $N^{-1/2}$; a practical value for N is then higher than 100 [19]. The computational time being approximatively proportional to N , the interest of choosing N as low as possible is obvious. A parametrical study is also useful here to optimize the computational time, without decreasing the accuracy of the result. This is addressed in the next subsection.

3.2. AMA validation

The first step is to try and find a value for γ . Let us use for this purpose the classic 1-D steady state diffusion/reaction model [24], which can be reduced from the general model proposed in Section 2.1. The 1-D reactant flux (Φ) at the interface can be analytically obtained [6] and writes

$$\Phi = \frac{D}{\delta_c} C_0 \frac{1}{1 + \frac{1}{Da}} \tag{11}$$

where $Da = k\delta_c/D$ is a Damköhler number. The evolution of the flux as a function of the Damköhler number is illustrated in Fig. 3b. For small Damköhler numbers, the flux is not a function of the reactivity (or of γ); this regime is called diffusion-limited. At the other limit ($Da \gg 1$), the consumed flux is only a function of the reactivity and the boundary layer concentration. A parameter variation study on γ in reaction-limited regime ($Da = 0.001$) is presented in Fig. 3a. It shows that if γ exists its value must be 0.8. In the reaction-limited regime, the normalized flux must display a variation proportional to $1/\gamma$ (from Eqs. (11) and (10)). This is verified and shows the existence of γ . The 2% uncertainty in reaction-limited regime is

352 molecules may be necessary to gasify the volume of one elementary
353 cube of solid. Using numerical simulation, it is impossible to have

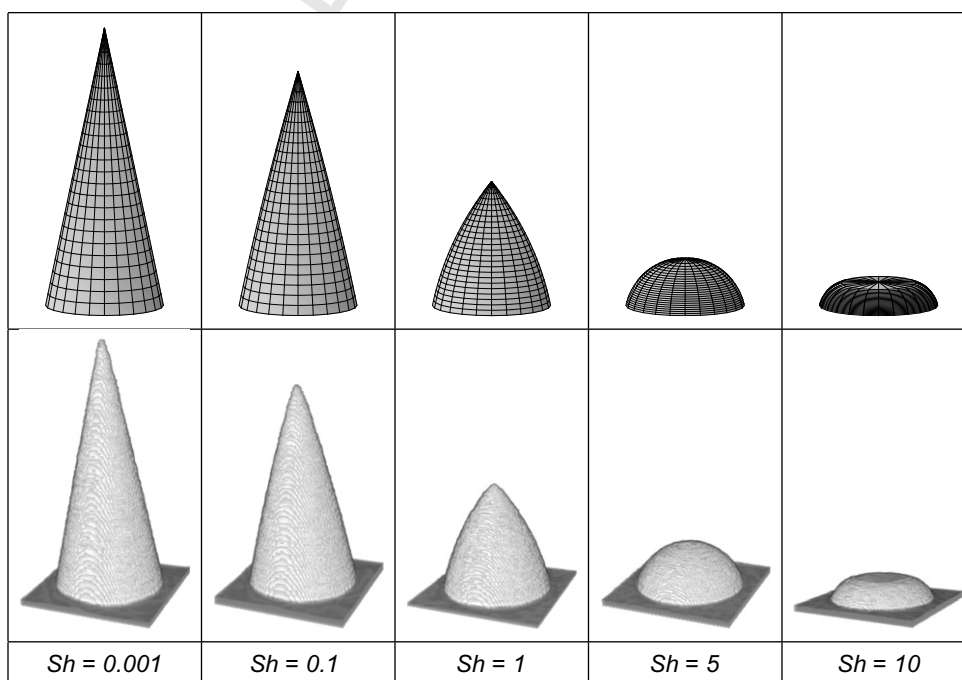


Fig. 4. Fiber morphology at steady state as a function of Sh (with $A = 5$): qualitative comparison of analytical solution (top) with AMA simulation (bottom).

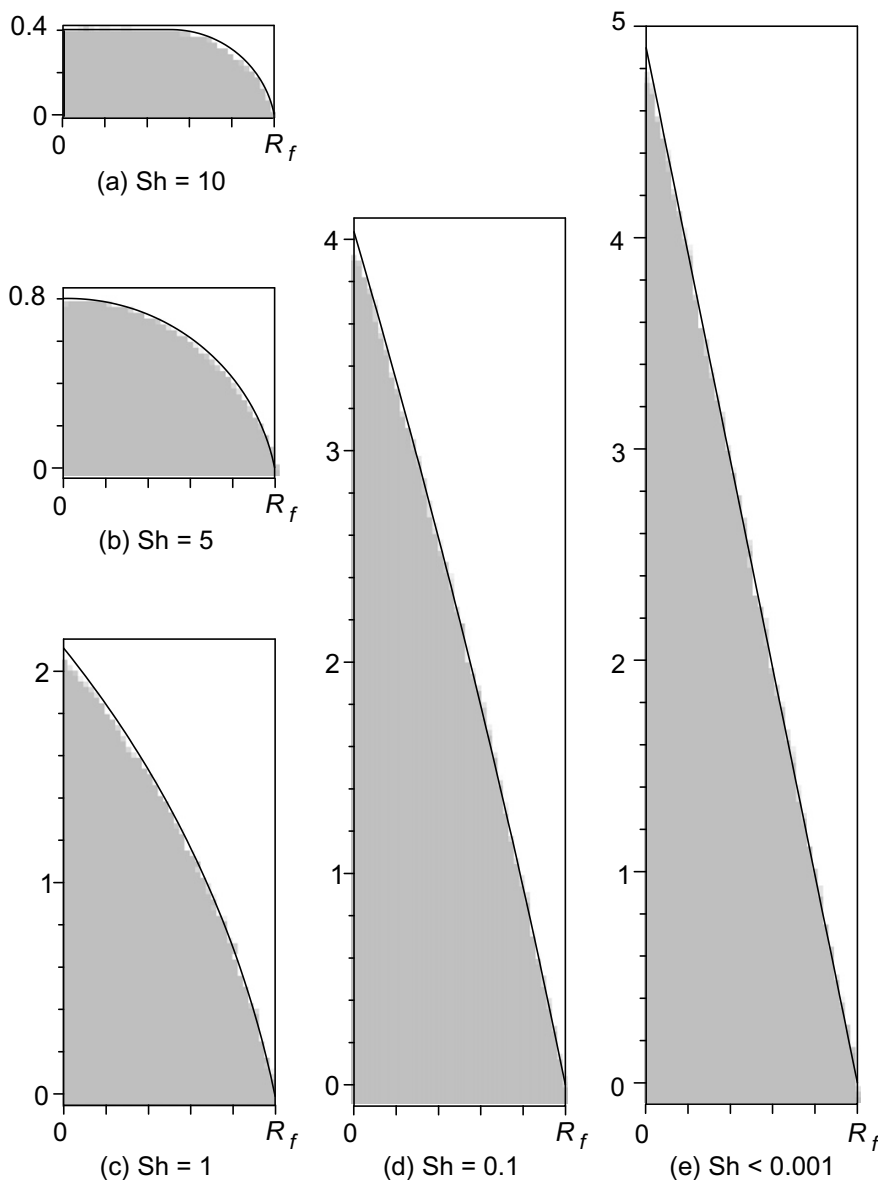


Fig. 5. Ablated fiber sections for different reaction/diffusion regimes: comparison of analytical (black lines) and numerical (grey-filled parts) results.

388 attributed to the Simplified Marching Cube description of the surface that saves computational time but is only a linear approxima- 408
 389 tion of the interface position, leading to a slight error on the 409
 390 estimation of the surface area. Using $\gamma = 0.8$, a parameter variation 410
 391 is carried out on Da . As shown in Fig. 3b, a correct agreement is obtained 411
 392 for all reaction–diffusion regimes. The uncertainty is found to 412
 393 be lower than the symbol size for any value of Da . This comes 413
 394 from the fact that the uncertainty decreases with Da because the 414
 395 diffusion process, which progressively dominates with the increase 415
 396 of Da , is independent of the local surface description. 416
 397

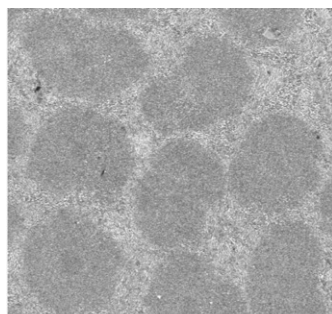
398 Random Walks have the particularity to converge on average at 417
 399 a rate proportional to the square root of the number of random 418
 400 drawings. The convergence has been obtained for $\Delta t_e \geq 100\Delta t$ 419
 401 for diffusion and $N \geq 10$ for reaction. In further simulations, these 420
 402 numerical conditions are systematically implemented using a pre- 421
 403 processor. Increasing the ratio between Δt_e and Δt , that is, decreasing 422
 404 Δr and increasing N , would lower the amplitude of the oscillations, but would dramatically enhance the computing time 423
 405 without changing the average value. For example, for a cubic cell 424
 406 of 100 pixel side length, it is more efficient and valid to use the 425

average flux as a reference value, using the following numerical 408
 parameters: $\Delta t_e = 100\Delta t$, and $N = 10$. 409

410 The quality of the moving interface description has also to be 411
 412 checked in 3D. The model of Section 2.2 has been solved using 413
 414 AMA, in all regimes for $A = 5$ (see Fig. 1c where $Sh \ll 1$, and Fig. 415
 416 4-bottom). These results are in qualitative agreement with the ana- 417
 418 lytical results of Figs. 1b and 4-top, respectively. To enable a quan- 419
 420 titative validation, sections of the analytical (black line) and of the 421
 422 numerical solutions (grey-filled part) are compared at Fig. 5. The 423
 424 overall agreement between the two solutions is excellent: the error 425
 is not larger than one pixel width. In the computed cases, the average horizontal section of the numerical cells is around 100 square pixels, which is a correct compromise between computational time and the quality of the interface description. The computational time is about 24 h with a 3.2GHz CPU computer.

4. Application to ablation 423

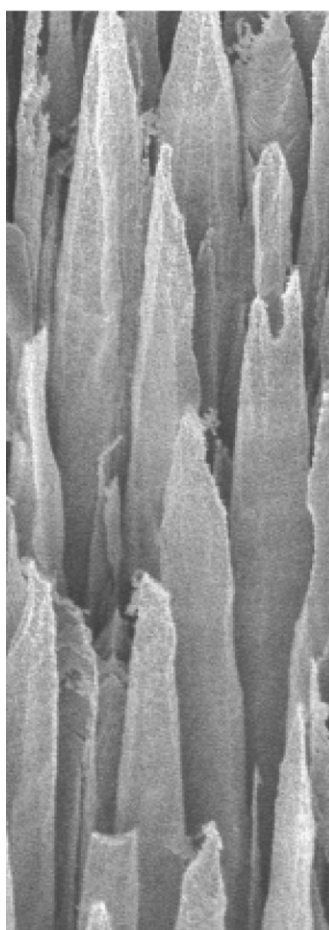
424 At microscopic scale, some roughness features take place on the 425
 425 stripped and pointed ablated fibers. In particular, ex-PAN fibers of



(a) Fibers sections : observation (SEM)



(b) Fiber section : model (AMA)



(c) Steady state (SEM)



(d) Steady state (AMA)

Fig. 6. Faceted fibers: comparison of experimental observations with a model of irregular fiber section.

3D C/C composites have been shown to be roughly conical but also faceted after ablation [25,6]. On Fig. 6c, some fibers from a 3D C/C oxidized under dry air at atmospheric pressure show such facets. The oxidation process as well as the composite are fully described in [7]. The ablation regime is shown to be reaction-limited ($Sh \ll 1$) [6]. In this case, when steady state is reached, fibers with circular cross-section display a regular conical shape (see Fig. 1b and c). Nevertheless, SEM (scanning electron microscopy) analyses of the fibers cross-section clearly show that it is irregular (see Fig. 6a). This may have an effect on the steady state geometry and behavior of the fibers. To verify this hypothesis, the irregularities of the fibers cross-section have been introduced in the model presented

in Section 2.2, as represented on Fig. 6b. The steady-state result of the simulation is presented on Fig. 6d¹. As a whole, the large facets which are experimentally observed on the fibers (from fiber tip to bottom) are qualitatively well reproduced. The numerical approach thus proves that they are originated from the irregularities of fibers sections. However, some facets, which are smaller, cannot be explained by this model. They may be linked to anisotropic nature of the graphitic carbon microstructure [26]. Indeed, a modified version

¹ A movie showing the transient regime of ablation, from a flat surface to the steady-state regime, is provided online (see Elsevier website).

446 of AMA accounting for anisotropic, orientation-dependent reactivity
 447 has allowed to show that the microstructure of a polycrystalline
 448 graphite acquires under ablation a characteristic roughness linked
 449 to its grain distribution [26].

450 5. Conclusions

451 A simulation tool useful for the modeling of surface roughness
 452 onset during ablation has been introduced in its context, pre-
 453 sented, and validated. First, a general model for receding surfaces
 454 under a first-order gasification process with a mass transport con-
 455 trolled by diffusion, which has been shown to explain well the
 456 ablation phenomenon, has been presented. To solve this model in
 457 the general case, numerical simulation tools are useful. AMA,
 458 which an efficient solution to solve reaction/diffusion problems
 459 with a receding surface based on a 3D numerical simulation code
 460 developed on a Monte-Carlo **Random Walk** principle with a Simpli-
 461 fied Marching Cube surface discretization scheme, has been pre-
 462 sented. AMA includes an automatic step refinement close to the
 463 wall that lowers the computational time. The reactivity is simu-
 464 lated using a sticking probability adapted to the **Random Walk**
 465 used (Brownian motion simulation technique). The resulting inter-
 466 face evolution in 3D has been validated by comparison to an ana-
 467 lytical model obtained in a previous study. As an application, the
 468 ablation of cylindrical fibers with a non-circular basis, embedded
 469 in a more reactive matrix, has been studied using AMA. An inter-
 470 pretation of the origin of the large facets experimentally observed
 471 on sharp ablated fibers has been proposed. The large facets basi-
 472 cally arise from the irregularities of fibers section which are inten-
 473 sified by ablation. This numerical simulation tool is then useful and
 474 efficient to analyse and understand surface roughness onset during
 475 ablation of composite materials.

476 As an opening, this code could be used as well to simulate other
 477 phenomena related to mass loss or mass deposition, including for
 478 example crystal growth, surface coating processes, sedimentation,
 479 and clogging that involve a similar physics but with a growing wall
 480 instead of a receding surface.

481 Acknowledgements

482 The authors wish to thank Y. Aspa (**LCTS-IMFT**), J.-F. Epherre, J.-
 483 M. Goyh  n  che, and G. Duffa (CEA) for fruitful discussions. The
 484 authors also wish to thank CNRS and CEA for a Ph.D. Grant to J.
 485 Lachaud.

Appendix A. Supplementary data

Supplementary data associated with this article can be found, in
 the online version, at doi:10.1016/j.commatsci.2008.07.015.

References

- [1] E. Fitzer, L.M. Manocha, Carbon Reinforcements and C/C Composites, Springer, 1998, p. 342.
- [2] G. Duffa, G.L. Vignoles, J.-M. Goyh  n  che, Y. Aspa, International Journal of Heat and Mass Transfer 48 (16) (2005) 3387–3401.
- [3] K. Kuo, S. Keswani, Combustion Science and Technology 42 (1986) 177–192.
- [4] S. Pestchanyi, V. Safronov, I. Landman, Journal of Nuclear Materials 329–333 (2004) 697–701.
- [5] M.R. Wool, Summary of experimental and analytical results, Technical Report SAMSO-TR-74-86, Passive Nosedip Technology Program (PANT), January 1975.
- [6] J. Lachaud, Y. Aspa, G.L. Vignoles, International Journal of Heat and Mass Transfer 51 (9–10) (2008) 2618–2627.
- [7] J. Lachaud, N. Bertrand, G.L. Vignoles, G. Bourget, F. Rebillat, P. Weisbecker, Carbon 45 (2007) 2768–2776.
- [8] G. Vignoles, J. Lachaud, Y. Aspa, Roughness Evolution in Ablation of Carbon-Based Materials: Multi-scale Modelling and Material Analysis, European Space Agency Special Publication, vol. 631, 2006, p. 8.
- [9] G. Vignoles, J. Lachaud, Y. Aspa, J.M. Goyh  n  che, Ablation of carbon-based materials: multiscale roughness modeling, to appear in Composites Science and Technology
- [10] Y. Aspa, M. Quintard, J. Lachaud, G.L. Vignoles, AIAA 2911 (2006) 52–64.
- [11] G.L. Vignoles, O. Coindreau, A. Ahmadi, D. Bernard, Journal of Materials Research 22 (6) (2007) 1537–1550.
- [12] I.C. Kim, S. Torquato, Journal of Applied Physics 68 (8) (1990) 3892–3903.
- [13] M.M. Tomadakis, S.V. Sotirchos, Chemical Engineering Science 48 (19) (1993) 3323–3333.
- [14] M. Plapp, A. Karma, Journal of Computational Physics 165 (2000) 592–619.
- [15] W.E. Lorensen, H.E. Cline, in: M.C. Stone (Ed.), SIGGRAPH'87 Proceedings of the ACM Computer Graphics, vol. 21, ACM Press, New York, 1987, pp. 163–169.
- [16] I.V. Katardjiev, G. Carter, M.J. Nobes, S. Berg, H.-O. Blom, Journal of Vacuum Science and Technology A 12 (1) (1994) 61–68.
- [17] J. Lachaud, Simulation of ablation of carbon-based composites, PhD thesis 3291, Bordeaux University, France, in English, 2006.
- [18] S. Torquato, I. Kim, Applied Physics Letters 55 (1989) 1847–1849.
- [19] J. Sall  s, J.F. Thovert, P.M. Adler, Chemical Engineering Science 48 (1993) 2839–2858.
- [20] G.L. Vignoles, Journal of Physics IV France C5 (1995) 159–166.
- [21] A. Gil, J. Segura, Computer Physics Communications 136 (2001) 269–293.
- [22] G. Federici, M. Mayer, G. Strohmayer, V. Chuyanov, C. Day, Journal of Nuclear Materials 337–339 (2005) 40–44.
- [23] A.S. Kim, H. Chen, Journal of Membrane Science 279 (1–2) (2006) 129–139.
- [24] J. Lachaud, G.L. Vignoles, J.M. Goyh  n  che, J.F. Epherre, Ceramic Transactions 191 (2006) 149–160.
- [25] J.C. Han, X.D. He, S.Y. Du, Carbon 33 (4) (1995) 473–478.
- [26] J. Lachaud, Y. Aspa, G. Vignoles, J.-M. Goyh  n  che, 3D Modeling of Thermochemical Ablation in Carbon-Based Materials: Effect of Anisotropy on Surface Roughness Onset, European Space Agency Special Publication, vol. 616, 2006, p. 10.